Low-noise phase-sensitive optical parametric amplifier with lossless local pump generation using a digital dither optical phase-locked loop

Research Article | Vol. 31, No. 22 / 23 Oct 2023 / Optics Express 36603
Optics EXPRESS

Low-noise phase-sensitive optical parametric amplifier with lossless local pump generation using a digital dither optical phase-locked loop

RASMUS LARSSON,[1,*] KOVENDHAN VIJAYAN,[1,2] JOCHEN SCHRÖDER,[1] AND PETER A. ANDREKSON[1]

[1] *Photonics Laboratory, Department of Microtechnology and Nanoscience, Chalmers University of Technology, SE - 412 96 Gothenburg, Sweden*
[2] *Now with Nokia Bell Labs, 600 Mountain Ave., Murray Hill, NJ 07974, USA*
[*] *rasmus.larsson@chalmers.se*

Abstract: The low noise figure of phase-sensitive amplifiers (PSAs) is attractive for optically pre-amplified measurement and communication systems. However, a major practical implementation difficulty pertains to the requirement of phase-locked signal, idler, and pump waves. Previously, injection locking to a co-propagating weak pump pilot or tapping portions of the received signal (lossy) for carrier re-generation have been used. Here we present a novel, lossless approach without any pump pilot, that generates a phase-locked receiver-local pump within the PSA using a digital dither-based optical phase-locked loop. We experimentally demonstrate a 2 dB noise figure with a low 0.3 dB penalty due to imperfect locking. By comparing the phase-locking performance in a PSA to that in a 50/50-coupler, we discuss and predict potential performance improvements connected to loop delay and laser phase characteristics.

1. Introduction

Phase-sensitive amplifiers (PSAs) offer several advantages over phase-insensitive amplifiers (PIAs) like the erbium-doped fiber amplifier (EDFA); they exhibit a theoretical 0 dB noise figure (NF) [1], can mitigate transmission nonlinearities [2,3] and are wavelength flexible with a potentially large gain bandwidth [4]. These appealing aspects of PSAs make them attractive for applications such as pre-amplification in free-space [5] and fiber-optical transmission links [2,6], all-optical phase and amplitude regeneration [7] and all-optical sampling [8,9].

PSAs, like other parametric amplifiers, rely on nonlinear interaction in either a three- [10] or four-wave mixing (FWM) process [11] where one or several pump waves exchange energy to weaker signal and idler waves. A common and practical setup for a PSA is the two-mode, degenerate pump configuration [4], where signal and idler waves are equally spaced apart in frequency around a central degenerate pump wave, see Fig. 1(a). The relative phase between these three waves determines the exchange of energy between them. The gain of such an amplifier can be written as [4]

$$G_{\mathrm{PSA}}(\delta\phi) = |\mu|^2 + |\nu|^2 + 2|\mu||\nu|\cos\delta\phi, \quad \delta\phi = \phi_s + \phi_i - 2\phi_p + \phi_\nu. \tag{1}$$

Here, $|\mu|^2 = G_{\mathrm{PIA}}$ is the PIA gain the signal wave experiences should the idler be absent at the amplifier input, $|\nu|^2 = G_{\mathrm{PIA}} - 1$, $\phi_{s,i,p}$ is the phase of the signal, idler, and pump waves respectively and ϕ_ν is a constant phase.

For the PSA to achieve phase-sensitive gain and reach the attractive <3 dB NF (lowest measured fiber-PSA NF: 1.1 dB [12]) the three waves need to be locked in phase at the PSA input. In the case of an optical link, while correlated signal, idler and pump waves are commonly produced in

#499280 https://doi.org/10.1364/OE.499280
Journal © 2023 Received 29 Jun 2023; revised 12 Sep 2023; accepted 16 Sep 2023; published 17 Oct 2023

Optics EXPRESS

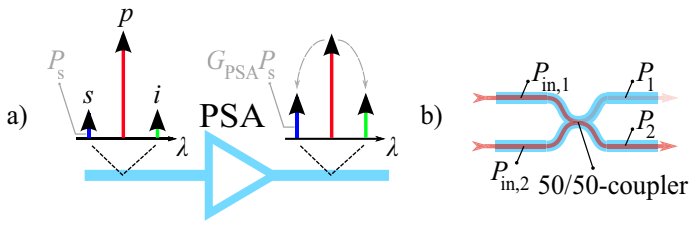

Fig. 1. a) PSA with input signal (of power P_s), idler, and pump waves. b) 50/50-coupler with input powers $P_{\text{in},1}$ and $P_{\text{in},2}$ and output powers P_1 and P_2.

the transmitter (Tx), usually by employing a copier scheme [4], it is practically difficult to create a correlated receiver (Rx)-side, high- power and quality, pump wave.

In previous PSA demonstrations, the pump was regenerated for the PSA, usually by co-propagating the Tx pump in the link along with the signal and idler for frequency-locking to an Rx-side slave laser using injection locking [13] or an optical phase-locked loop (OPLL) [14]. Other approaches involve tapping part of the received signal as carrier reference for an OPLL [15]. In addition, another OPLL has been used to maintain the phase locking. In either solution, the power in a co-propagating pump carrier or the tapped portion of the signal will negatively impact the black-box NF of the PSA.

Here we demonstrate a method that eliminates the need for co-propagating a pump or tapping the received signal before amplification. It uses phase dithering and a field-programmable gate array (FPGA) to control the phase and frequency of an Rx-side pump laser to directly maximise the PSA gain. Our OPLL design is closely related to that of previous works focused on local oscillator phase locking for homodyne coherent reception [16–19]. Here, just like in [18] we add an external phase modulator in addition to the frequency control of the Rx-side laser, the difference being that the PSA itself is used to generate the error signal instead of the phase-sensitive process of coherent reception.

While the PSA performs coherent superposition of waves in the spectral domain (via FWM), a 50/50-coupler (50/50) coherently superposes spatially separate waves, see Fig. 1(b). Similarly to Eq. (1), the 50/50 output power P_2 (in Fig. 1) can be written as

$$P_2(\Delta\phi) = \frac{1}{2}[P_{\text{in},1} + P_{\text{in},2} + 2\sqrt{P_{\text{in},1}P_{\text{in},2}}\cos\Delta\phi] \tag{2}$$

where $P_{\text{in},1}$ and $P_{\text{in},2}$ are the powers of the two input waves and $\Delta\phi$ is the relative phase between them. The near-identical phase dependence between Eq. (1) and (2) indicates that locking signal, idler, and pump waves in a PSA is virtually the same challenge as phase-locking the two inputs of a 50/50. This is the premise of coherent combining [20], homodyne reception, and frequency locking of lasers [21].

Because of its similar phase dependence to the PSA and its simplicity, the 50/50 is used in this work to investigate and understand the OPLL performance under different conditions such as received optical power and loop delay. This is done both experimentally and via numerical simulations. The results following this are then used to predict the performance of the PSA under improved conditions, specifically for reduced loop delay and phase noise of the involved lasers.

Note that this work is an extension of [22] which was presented at Optical Fiber Communication Conference (OFC) in 2023 and where this concept was first presented. In this extension we discuss further details on the optical phase locked loop, what aspects affect its performance and what impact it has on the PSA. We also include the 50/50 phase-locking comparison for OPLL performance evaluation and PSA improvement predictions. In addition, bit error rate (BER) curves have been re-measured with improved results. Also, this work focuses on classical optical communication links and hence, is not in the context of quantum mechanics PSAs as in [23].

Optics EXPRESS

In section 2, we present the OPLL achieving the phase lock. The operation of the OPLL on the 50/50 is experimentally and numerically investigated in section 3. The experimental setup for phase-sensitive pre-amplification and the relevant results are presented in section 4. In section 5 we evaluate the OPLL performance on the PSA and discuss the potential of the local pump PSA under improved conditions. Further discussion and conclusion are given in section 6.

2. Optical phase locked loop

To achieve phase sensitive gain in a PSA or coherent superposition in a 50/50, the phases and thereby the frequencies of all input waves must be locked to each other. As was mentioned, for the PSA we focus on we can expect a correlated signal and idler wave while the pump, which is produced at the Rx, will exhibit uncorrelated phase noise and frequency drift (and a possible Doppler shift). The task of the OPLL is therefore to compensate any relative frequency drift or phase noise between these three waves, or in the case of the 50/50, two uncorrelated input waves.

Our OPLL, presented in Fig. 2(a), is applied both to the PSA system in Fig. 2(b) and the 50/50 in Fig. 2(c), where optical amplification ensures similar noise performance in both systems. The OPLL achieves frequency control via current control of a local laser (Rx pump for PSA) and phase control using an external electro-optic phase modulator (ϕ-mod). After these controls are applied the residual phase error ϕ_e (= $\delta\phi, \Delta\phi$ from Eq. (1), (2)) between the waves is minimized during successful locking.

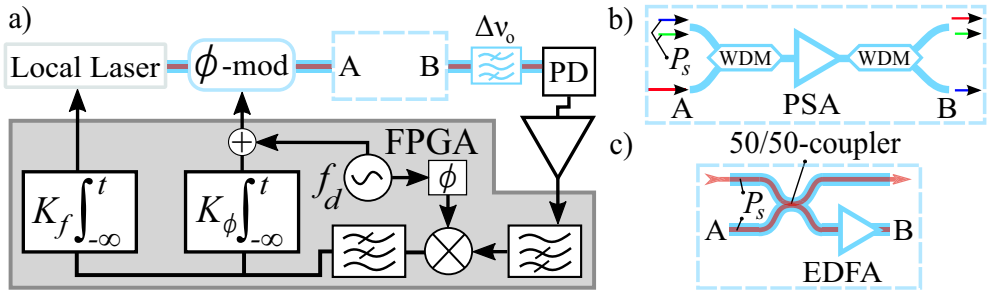

Fig. 2. a) Schematic of the OPLL operating on optical system in the dashed box. $\Delta\nu_o$: optical bandpass filter with bandwidth $\Delta\nu_o$. b) PSA sub-system. WDM: wavelength division multiplexer. c) 50/50 sub-system.

Continuous tracking and minimization of the phase error requires an error signal proportional to ϕ_e to be generated. This is done by applying a small single-tone, sinusoidal phase pertubation (dither) $\phi_d \cos(2\pi f_d t)$ in the phase modulator with magnitude ϕ_d and frequency f_d (t is time). Via the phase dependence in Eqs. (1) and (2), the dither produces an optical error signal proportional to the phase error ϕ_e and oscillating at f_d, contained in the power detected in the PD [17]. The electrical signal is then amplified in a low noise amplifier before being fed into a 125 MS/s, 14-bit Red Pitaya field-programmable gate array (FPGA) [24], where sampling, filtering and demodulation (at f_d) is carried out. The resulting baseband signal is proportional to $J_1(\phi_d)P_s \sin\phi_e$ which for small phase errors is proportional to the phase error: $\sin\phi_e \approx \phi_e$. Here, $J_m(x)$ is the Bessel function of first kind and order m and P_s is the input signal/idler power for the PSA or power per input for the 50/50 ($P_s = P_{\text{in},1} = P_{\text{in},2}$). Finally, ϕ_e is minimized as the baseband signal is sent to two separate integrators with equivalent total loop gains k_ϕ and k_f for phase control in the electro-optic phase modulator and for frequency control of the local laser, respectively.

Note that due to the implementation of the phase modulator, Whenever its driving voltage limit is reached 2π-phase jumps are carried out to maintain phase-lock. The effect of these ($\sim$ 1

Optics EXPRESS

μs duration) phase jumps can be engineered away, e.g., by using an additional phase modulator as in [25] and hence do not pose a fundamental limitation.

While the choice of ϕ_d, k_ϕ and k_f will affect the residual phase error of the OPLL and hence its performance, f_d is typically chosen large enough (here $f_d = 31.25$ MHz) for the OPLL to differentiate it from the phase noise that should be compensated.

2.1. Residual phase errors and locking efficiency

Although the OPLL design minimizes ϕ_e, it will have a residual non-zero value with associated variance $\sigma^2_{\phi_e}$ that will impact the quality of the phase locking and the final PSA performance. Any phase noise beyond the loop bandwidth B_L or system noise within the equivalent noise bandwidth B_n, will add contributions σ^2_ϕ and σ^2_{N}, respectively, to $\sigma^2_{\phi_e}$. Additionally, the phase dither itself constitutes another contribution $\sigma^2_{\phi_d} = \phi_d^2/2$. Other smaller contributors to $\sigma^2_{\phi_e}$ are the impact of finite, discrete frequency resolution f_{res} in the digital frequency control $\sigma^2_{f_{\mathrm{res}}}$ and the phase error due to frequency drift $\sigma^2_{\Delta f}$ (potentially limiting for large Doppler shifts).

The exact variances of all contributions are covered in Supplement 1 upon which the numerical simulations are based. Meanwhile, for the purpose of a qualitative understanding, simpler expressions for the two dominating contributions are obtained assuming Lorentzian phase noise of linewidth $\Delta\nu$, white system noise, small frequency drifts and zero loop delay, for which

$$\sigma^2_\phi = \frac{\Delta\nu}{B_L}, \quad \sigma^2_{\mathrm{N}} = \mathrm{SNR}^{-1}_{\mathrm{OPLL}} = \frac{S_n(a)B_n}{a^2 J_1(\phi_d)^2 P_s^2}, \quad B_L = \frac{k_\phi}{2\pi}, \quad B_n = \frac{k_\phi}{4} \tag{3}$$

where $a = 1$ for the 50/50 and $a = 2$ for the PSA, $\mathrm{SNR}_{\mathrm{OPLL}}$ is the OPLL error signal to noise ratio (SNR) and $S_n(a) = \frac{1}{2a}(F_n h\nu)^2\Delta\nu_o + 2aP_sF_nh\nu$ is the dominating system noise power spectral density (PSD) due to the optical amplification. Here, F_n is the EDFA or PIA NF (ideally equal to 2), ν the optical frequency, h Plank's constant and $\Delta\nu_o$ is the optical filter bandwidth.

From Eq. (3) we note that suppressing σ^2_ϕ implies either increasing k_ϕ or improving the phase noise characteristics of the involved lasers while σ^2_{N} may be decreased by reducing k_ϕ or by increasing either the received power P_s or ϕ_d. For a given P_s and $\Delta\nu$ however, minimizing σ^2_{N} opposes simultaneous minimization of σ^2_ϕ or $\sigma^2_{\phi_d}$ via the OPLL parameters ϕ_d and k_ϕ alone. For a minimal phase error $\sigma^2_{\phi_e} \approx \sigma^2_{\phi_d} + \sigma^2_\phi + \sigma^2_N$ and best OPLL performance there exists a trade-off between the different contributions and the OPLL parameters ϕ_d and k_ϕ (and k_f for non-negligible drift) must therefore be optimized.

In a PSA, the impact a residual phase error has is the reduction of phase-sensitive gain and subsequent NF degradation. The important quality metric can therefore be defined in terms of the locking efficiency $\eta(\phi_e)$

$$\eta(\phi_e) = \frac{1}{2}[1 + \cos\phi_e] = \frac{P_2(\phi_e)}{P_2(\phi_e = 0)} \approx \frac{G_{\mathrm{PSA}}(\phi_e)}{G_{\mathrm{PSA}}(\phi_e = 0)}, \quad \langle\eta\rangle = \frac{1}{2}[1 + e^{-\sigma^2_{\phi_e}/2}] \tag{4}$$

where for the PSA it is assumed $G_{\mathrm{PIA}} \gg 1$. Here $\langle\eta\rangle$ is the time-average locking efficiency, its relation to $\sigma^2_{\phi_e}$ is verified in Supplement 1. The PSA NF degradation induced by imperfect locking is then $F_\eta = 1/\eta$ and governs the impact the OPLL has on the final bit error rate $\mathrm{BER} = \frac{1}{2}\mathrm{erfc}(\sqrt{\eta E_b/N_o})$, where E_b/N_o is the energy per bit to noise power spectral density ratio of the received quadrature phase shift keyed (QPSK) communication data when $\phi_e = 0$.

3. Locking efficiency of the 50/50-coupler

The simplicity of the 50/50 compared to the PSA makes it a practical testing platform for the OPLL. Thanks to its small size it also allows operating the OPLL at much shorter loop delays than with the 600 m long highly nonlinear fiber PSA. The significant PSA length is further

Optics EXPRESS

recognized as a potential limitation to OPLL performance since large loop delays in general are problematic in control systems. As such, to investigate the effect of loop delay, the time-average locking efficiency was both experimentally measured and simulated for different excess loop delays τ_e and the received power per input P_s, using the 50/50.

The results are shown in Fig. 3(a)-(d), where, for each investigated combination of P_s and excess loop delay τ_e the OPLL parameters (k_ϕ, k_f and ϕ_d) were optimized to maximize $\langle\eta\rangle$.

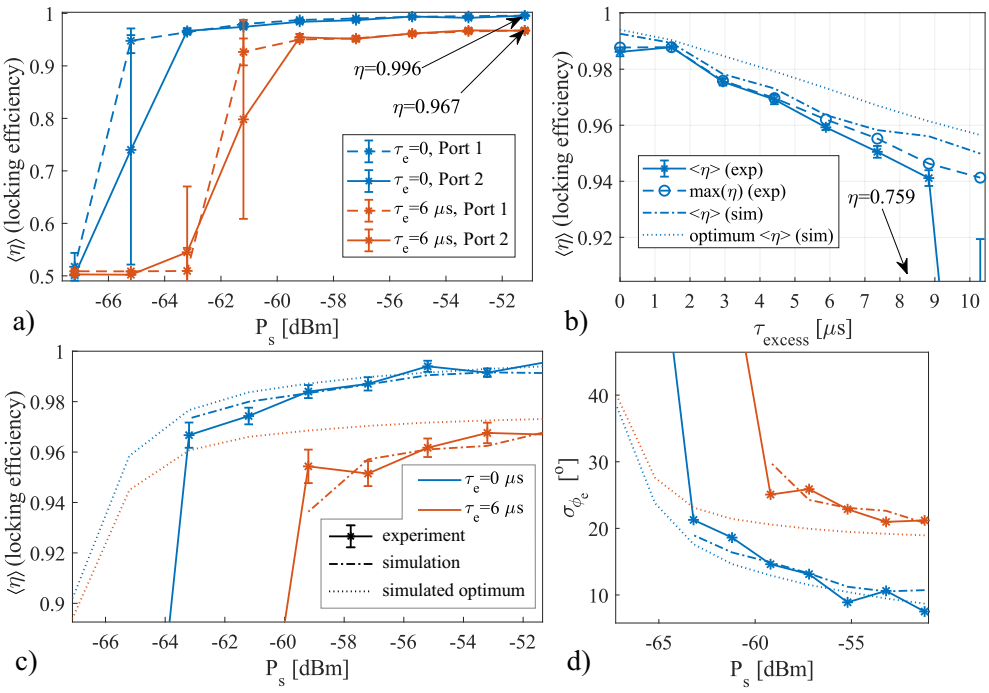

Fig. 3. η and σ_{ϕ_e} of the 50/50 with standard deviation error bars. a) Measured $\langle\eta\rangle$ vs. P_s for different excess loop delay τ_e with error signal read-out at output port 1 (destructive) or 2 (constructive). b) Measured and simulated $\langle\eta\rangle$ vs. τ_e at $P_s = -51.6$ dBm. c) Measured (same as in a)) and simulated $\langle\eta\rangle$ vs. P_s for error read-out at port 2 and different excess loop delay τ_e. d) Corresponding phase error standard deviation σ_{ϕ_e} from c) but without error bars.

The measured $\langle\eta\rangle$ was obtained using the setup in Fig. 2(a) and (c) during coherent combining of light from a Thorlabs ULN distributed fiber Bragg grating laser with external feedback cavity (as the local laser) and an NKT fiber laser, both emitting at wavelength $\lambda = 1550.5$ nm with sub-kHz linewidths. The locking efficiency was measured over 20 batches as $\langle\eta\rangle = P_2/2P_s$ with P_2 being the output port of constructive interference (see Fig. 1(b)), whose power was recorded using a power meter. P_s was swept using a variable optical attenuator (VOA) inserted before the EDFA (with 4 dB NF) and different excess loop delays τ_e were introduced by fiber delays between the EDFA and the optical filter ($\Delta\nu_o = 0.22$ nm). Total loop delays were $\tau_\phi = \tau_{\phi_0} + \tau_e$ and $\tau_f = \tau_{f_0} + \tau_e$, where $\tau_{\phi_0} = 1.5$ μs and $\tau_{f_0} = 0.75$ μs were the delays imposed by the FPGA and radio frequency (RF) system for the phase and frequency control respectively (see Supplement 1). Meanwhile, the frequency resolution f_{res} was fixed to 930 Hz.

Simulated $\langle\eta\rangle$ (dashed) were calculated from the recorded OPLL parameter values (k_ϕ, k_f and ϕ_d) used in the experiment. For simulated optimum $\langle\eta\rangle$ (dotted) the OPLL parameters were numerically optimized for minimized phase error variance, while simultaneously fulfilling phase margin and SNR conditions to ensure stability (see Supplement 1).

Optics EXPRESS

From Fig. 3 it is clear that increasing loop delay has a detrimental effect on the OPLL performance and maximum achievable $\langle\eta\rangle$. In a) the measured $\tau_e = 6$ μs case suffers both a reduction to $\langle\eta\rangle$ vs. the measured $\tau_e = 0$ case (from 0.996 to 0.967) as well as a sensitivity reduction, i.e. increased P_s cut-off for when the OPLL loses phase-lock. This cut-off in P_s was also observed to vary depending on the error read-out port, which is expected as the signal-optical noise beating at the PD depends on the signal power, which in the destructive port is negligible. In b) a steady decline in maximum $\langle\eta\rangle$ is observed with increased τ_e both for experiment and simulated optimum $\langle\eta\rangle$. Increased instability as well as difficulties to achieve and maintain phase-lock was experienced for larger τ_e in addition to the reduced $\langle\eta\rangle$, to a point where locking was lost occasionally for the largest investigated τ_e ($\eta = 0.759$).

Agreement between numerically calculated $\langle\eta\rangle$ and measurement is good throughout Fig. 3(b-d). Here, the simulated optimum $\langle\eta\rangle$ appears not far above the experimentally obtained efficiencies, indicating a close to optimum performance of the experimental setup. What the simulation appears failing to capture is the increased P_s cut-off due to added excess loop delay. Additional stability conditions are most likely needed for improved comparison.

In general, it is known that large loop gains in combination with large loop delays causes control system instability. The reason for reduced $\langle\eta\rangle$ with increasing delay is therefore explained by the reduced maximum allowable loop gain for maintained stability, which in turn results in a larger σ_ϕ^2 and worse $\langle\eta\rangle$ than in the $\tau_e = 0$ case. Additional simulations showing the individual contributions to $\sigma_{\phi_e}^2$, presented in Supplement 1, support this result.

Lastly, in the case of no excess delay, $\tau_e = 0$, measurement results show that the OPLL achieves locking efficiencies >0.99, corresponding to NF sensitivity penalties <0.05 dB for a PSA. This experimentally verifies the potential of the OPLL, at least for the 50/50 case.

4. Local pump phase sensitively pre-amplified receiver experiment

Having successfully demonstrated coherent combining using the OPLL we now use it here to demonstrate local pump generation in an Rx-side phase sensitively pre-amplified receiver of optical communication data.

In order for a PSA to amplify a signal wave carrying data encoded in its phase ϕ_s, the phase $\delta\phi$ in Eq. (1) must still be zero. Practically one achieves this by ensuring that the idler phase ϕ_i carries the conjugated data signal to cancel out the influence of the data modulation on the PSA operation. Naturally, the idler wave must therefore be created at the Tx where the data is available and subsequently transmitted alongside the signal in the link.

In our experimental setup, depicted in Fig. 4(a), a signal wave carrying a 10 GBaud QPSK data signal is combined in a WDM with an amplified pump wave from the NKT fiber laser. The conjugated idler is then produced by copying the signal using FWM in a highly nonlinear fiber, denoted copier. Note that apart from the data, any phase noise or frequency drift of the signal is also conjugated onto the idler and therefore cancelled out at the PSA. The NKT pump phase noise and frequency drift ϕ_{NKT} is however introduced in the idler as: $\phi_i = 2\phi_{\mathrm{NKT}} - \phi_s$.

After the copier, the pump wave is filtered away using a WDM before signal and idler waves (of equal powers) are sent through a VOA, representing a lossy channel. At the Rx side, the signal and idler are combined with an amplified pump wave (29.4 dBm) from the Thorlabs ULN external fiber-Bragg grating cavity laser with phase ϕ_{ULN}. The signal and idler experience gain in the 600 m long highly nonlinear fiber-PSA according to Eq. (1), where now $\delta\phi = 2(\phi_{\mathrm{NKT}} - \phi_{\mathrm{ULN}}) + \phi_\nu$. The signal is then separated using an optical filter ($\Delta\nu_o = 0.22$ nm) before detection in an intradyne coherent receiver and sampling in a real-time oscilloscope for offline processing and BER analysis. Observe that the reception is, in principle, lossless since no signal or idler power needs to be tapped at the input of the amplifier, which would degrade the "black-box" NF.

The offline digital signal processing involved: resampling, IQ-imbalance and frequency offset compensation, constant modulus, and carrier phase estimation as described in [26]. A 10% tap

Optics EXPRESS

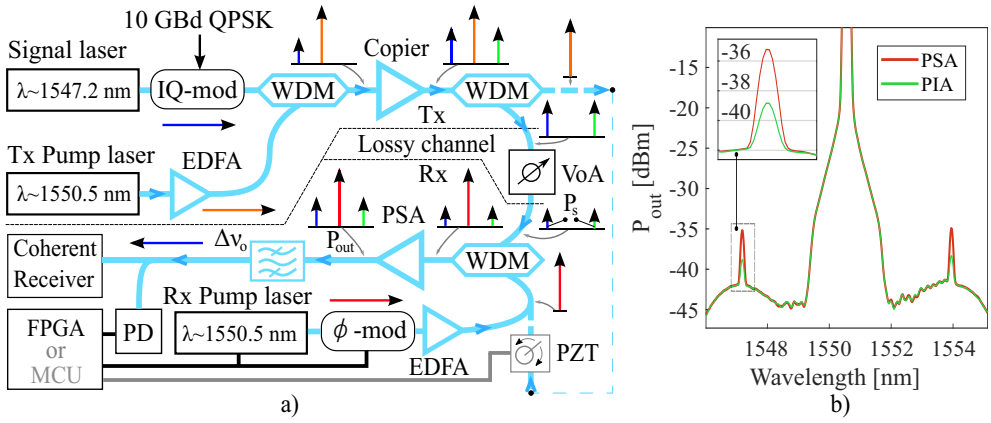

Fig. 4. a) Transmission system with a Tx-side copier stage, a lossy channel, and an Rx-side PSA with either a loop-controlled Rx- or recycled Tx pump. PZT: Piezo-electric transducer, VoA: Variable optical attenuator, MCU: Micro-control unit. b) PSA and PIA output spectra captured by an OSA at $P_s = -56$ dBm.

before coherent reception provided the optical error signal to the OPLL. Polarization controllers throughout the system were used to align the polarizations of all waves at all points.

The received signal/idler power P_s was swept by changing the VOA attenuation and for each P_s the OPLL parameters k_ϕ, k_f and ϕ_d were optimized to maximize the output signal power monitored using an optical spectrum analyzer (OSA). Meanwhile, f_{res} was halved to 465 Hz to keep the same effective resolution of 930 Hz (due to $2\phi_p$ in Eq. (1)).

For comparison, PIA measurements were performed where the idler was removed from the PSA input. Similarly, to compare with an ideal PSA, a reference measurement was performed where the correlated pump wave from the Tx was phase-aligned using a PZT (controlled by a micro-control unit (MCU)) and used to pump the PSA.

4.1. Results

Typical PSA output power OSA traces are presented in Fig. 4(b) (here for $P_s = -56$ dBm) where the phase-sensitive operation of the PSA is observed in the added gain compared to the PIA case.

From the received power (measured using a power meter) and the optical signal to noise ratio (OSNR) at the PSA output (measured with the OSA), the gain and noise figure were estimated as; for the local pump-locked PSA (PSA_{LP}) $G_{\text{LP}} = 20$ dB and $F_{\text{LP}} = 2$ dB, the reference PSA (PSA_{REF}) $G_{\text{REF}} = 20.5$ dB and $F_{\text{REF}} = 1.5$ dB and for the PIA $G_{\text{PIA}} = 14.5$ dB and $F_{\text{PIA}} = 4.5$ dB. Note that these NFs are w.r.t the total received power P_r, which is always (in this work) $P_r = 2P_s$ for the PSA and $P_r = P_s$ for the PIA. Again the less than 3 dB PSA NF and performance improvement over the PIA indicate phase-sensitive operation of the PSA and successful phase locking of the Rx pump laser.

Presented in Fig. 5 are the BER curves for the PSA_{LP}, PSA_{REF}, and PIA cases along with an EDFA pre-amplified receiver with $F_{\text{EDFA}} = 4$ dB as well as theoretical PSA and PIA BER-curves. BERs are plotted vs. P_r, in consistence with [22]. Experimental curves are averaged from the 10 best (out of 30) measurement batches of 500 k symbols at each P_r. No 2π-phase jumps occurred during these batches.

Here we note a close to 3 (2.95)dB sensitivity improvement for the PSA_{REF} vs. the PIA w.r.t. P_r. The power difference of the reference case and the PIA case w.r.t. the two corresponding theoretical curves are both 2.2 dB for BERs below 0.03. The sensitivity penalty at different BER for the PSA_{LP} can be read from the sub-figure in the right of Fig. 5 w.r.t. PSA_{REF} in yellow

Optics EXPRESS

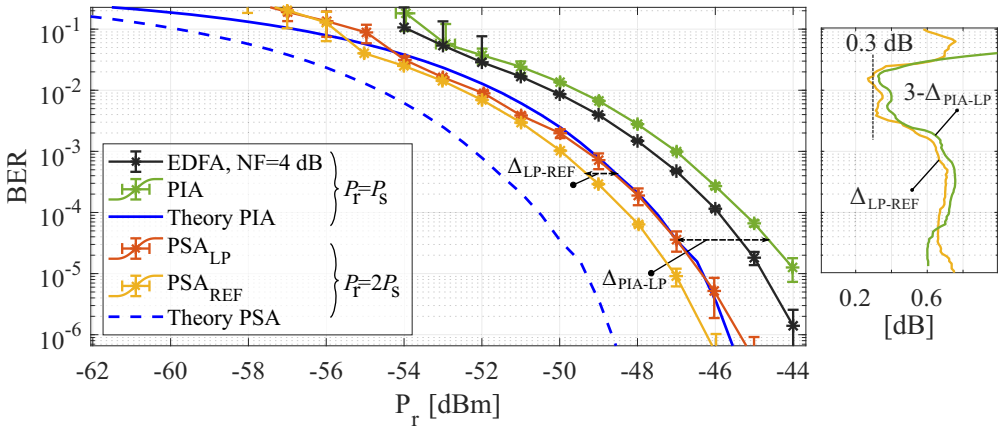

Fig. 5. a) Theoretical and measured BER curves, including standard deviation error bars, vs. total received power P_r (including idler, i.e. $P_r = 2P_s$, in case of PSA). Theory PSA and PIA NFs are 0 dB and 3 dB respectively. The sensitivity penalty of PSA_{LP} w.r.t. PSA_{REF} and PIA is emphasized in the sub-figure to the right.

and the PIA when shifted 3 dB to the left, in green. For $P_r > -51$ dBm the PSA_{LP} sensitivity penalty is ≈ 0.7 dB vs. PSA_{REF} and the 3dB-shifted PIA. For -54 dBm $\leq P_r \leq -51$ dBm the corresponding sensitivity penalty is instead ≈ 0.3 dB. The 0.05 dB power difference between the two curves of the sub-figure of Fig. 5 implies a locking efficiency of ≈ 0.99 for PSA_{REF} which incorporates both polarization misalignment and the residual phase error of the slow MCU-based PLL. The PSA_{LP} sensitivity degradation vs. PSA_{REF} is therefore solely due to imperfect phase locking of the Rx pump laser whereas penalties vs. the 3dB-shifted PIA also accounts for polarization misalignment.

At higher BERs the phase-estimator of the post-processing no longer converges and outputs erroneous values. Saturation issues within the OPLL is likely the cause for the higher PSA_{LP} sensitivity penalty at $P_r > -51$ dBm, hence the BER at -54 dBm $\leq P_r \leq -51$ dBm (-57 dBm $\leq P_s \leq -54$ dBm) provides a more relevant result of the OPLL performance. In the next section, this 0.3 dB penalty is further discussed and via simulations observed to improve when either the significant loop delay (600m PSA) or the laser phase noise is reduced.

5. PSA locking efficiency

For the investigated PSA, phase-locking is achieved when the Tx and Rx pump phases coincide $\delta\phi = 2(\phi_{NKT} - \phi_{ULN}) = 0$ (neglecting constant phases), hence the coherence of these lasers (the NKT and ULN lasers) govern the phase $\delta\phi$, just as they did $\Delta\phi$ in the coherent combining investigation. The phase noise PSDs of the two lasers, characterized using delayed (80 km) self-heterodyne interferometry [27], are shown in Fig. 6(a) alongside an asymptotic Lorentzian PSD with $\Delta\nu = 60$ Hz. A typical relative frequency drift of these lasers is also presented in Fig. 6(b) with corresponding statistics in Fig. 6(c) which indicate a maximum drift of about 1.5 MHz/s.

However, due to the factor of 2 in $\delta\phi = 2(\phi_{NKT} - \phi_{ULN})$ it follows that the phase noise PSDs of the lasers are experienced 4 times stronger by the PSA. Therefore, σ_ϕ^2 (as well as $\sigma_{\Delta f}^2$) is 4 times larger for the PSA case than for the 50/50. Any phase variation on the PSA input is doubled compared to the 50/50, making phase-locking more challenging. This problem is further exacerbated with increasing loop delay as the need for larger loop gains in conjunction with

Optics EXPRESS

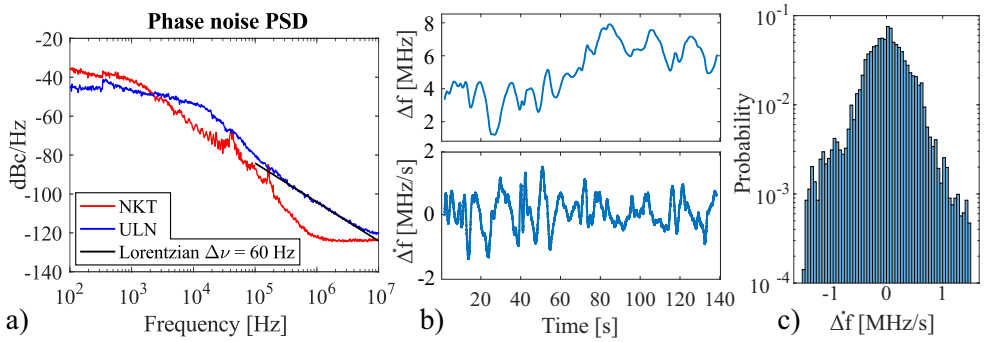

Fig. 6. a) Thorlabs ULN (Rx pump), NKT (Tx pump) and asymptotic Lorentzian phase noise PSDs. b) Typical relative frequency drift between the ULN and NKT lasers. c) Probability density of the drift $\dot{\Delta f}$ in b).

significant delay renders the OPLL more unstable. Meanwhile, the doubling of ϕ_d and f_{res} can simply be canceled by halving these OPLL parameters.

For the PSA, comparison between experimentally estimated $\langle\eta\rangle$ and simulated optimum $\langle\eta\rangle$ are shown in Fig. 7(a) vs. P_s. The locking efficiency $\langle\eta\rangle$ was extracted from the BER curves of Fig. 5, using the PIA results to estimate E_b/N_0 for $\phi_e = 0$. The locking efficiency was also estimated from the OSA gain measurements using Eq. (1). The BER-estimated $\langle\eta\rangle$ shows the short term efficiency during the 10 best (out of 30) measured symbol batches (of $\sim 1\mu$s duration) whereas the OSA-estimated $\langle\eta\rangle$ was averaged over the OSA sweep time (of $\sim$ 1s duration).

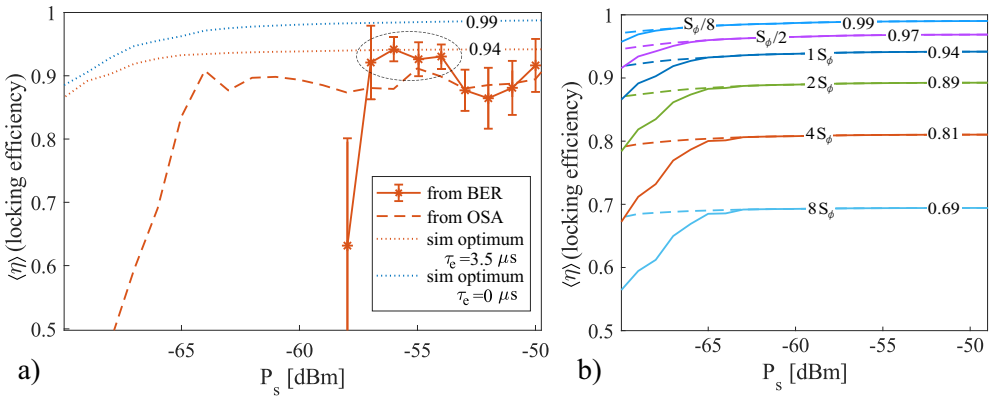

Fig. 7. a) Estimated PSA_{LP} $\langle\eta\rangle$ vs. P_s from both BER and OSA gain measurements with standard deviation error bars as well as the simulated optimum $\langle\eta\rangle$ for both the PSA delay $\tau_e = \tau_{\text{PSA}} \approx 3.5$ μs and $\tau_e = 0$. b) Simulated optimum $\langle\eta\rangle$ at $\tau_e = \tau_{\text{PSA}}$ for different phase noise PSD powers S_ϕ where the $1S_\phi$ curve is the same as the orange dotted line in a). Dashed curves are without the imposed SNR stability condition.

As expected, the BER-estimated $\langle\eta\rangle$ follows the same trend as the sensitivity penalty of the subfigure in Fig. 5 and within the marked region (-57 dBm $\leq P_s \leq -54$ dBm) $\langle\eta\rangle$ is close to the simulated optimum. This indicates that the PSA experiment performs close to optimal for the given conditions. The OSA-estimated $\langle\eta\rangle$ presents a better estimate of the time-average locking efficiency and is, as expected, slightly lower than that of the BER. It also provides a broader P_s measurement range than the BERs (limited to $P_s < -58$ dBm) and indicates a P_s cut-off of the PSA at -64 dBm. The simulated case of $\tau_e = 0$ further suggests that a 0.99 locking efficiency

Optics EXPRESS

is achievable for a significantly shorter PSA. As sensitivity was observed to degrade with τ_e in Fig. 3(a) we can expect also an improved sensitivity below $P_s = -64$ dBm in the $\tau_e = 0$ case.

In case, when the PSA for performance reasons cannot be made shorter, it is of interest to know the requirement on the lasers to improve σ_ϕ^2 and thereby the locking performance. A simulation was performed and is presented in Fig. 7(b), showing simulated optimum $\langle\eta\rangle$-curves vs. P_s for different phase noise PSD strengths. Here, $1S_\phi$ is the combined NKT and ULN phase noise PSD and different magnitudes of S_ϕ is equivalent to different magnitudes of combined linewidth $\Delta\nu$. From this result, we can predict that a combined phase noise PSD of 8 times lower power ($\Delta\nu$ on the order of 10 Hz) is required to achieve $\langle\eta\rangle \approx 0.99$ given a PSA delay $\tau_e \approx 3.5$ μs.

In case a significantly shorter PSA is realizable, for instance by implementing it on a photonic integrated circuit [28], the resulting $\tau_e = 0$ would alleviate the laser requirements for high $\langle\eta\rangle$. With $\tau_e = 0$ the relaxed laser requirements would instead be given by the simulation in Fig. 8(a).

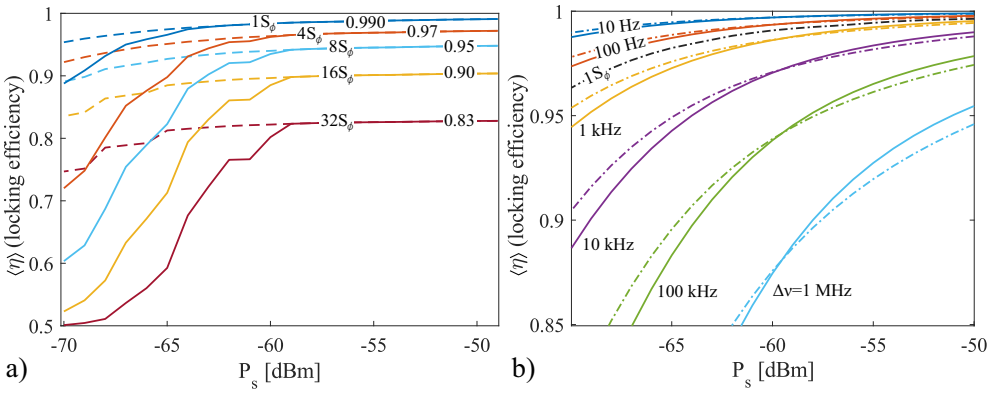

Fig. 8. a) Simulated optimum $\langle\eta\rangle$ at $\tau_e = 0$ for different phase noise PSD powers. Dashed curves are without the imposed SNR stability condition. b) Analytical optimum $\langle\eta\rangle$ vs. P_s for zero loop delay and negligible drift and frequency resolution. Dash-dot lines are the PSA and solid lines are the 50/50, at different Lorentzian linewidths alongside the laser phase noise PSD case $1S_\phi$ of the lasers used here ($\Delta\nu \approx 350$ Hz).

Here, the characteristics of the lasers used in this work ($\Delta\nu \sim 100$ Hz) are predicted to achieve $\langle\eta\rangle \geq 0.99$. Intuitively, minimizing the PSA length improves performance and the simulated 0.99 efficiency indicates the potential of the local pump OPLL approach for short PSAs. Yet, worse-performing lasers are not recommended to maintain high locking efficiency, at least for the base delays τ_{ϕ_0} and τ_{f_0} imposed by the Red Pitaya FPGA and RF low-noise amplifiers used here.

In case the complete loop delay, frequency drift and resolution are negligible and the laser phase noise is purely Lorentzian, the optimum OPLL parameters are found analytically when $\sigma_{\phi_d}^2 = \sigma_\phi^2 = \sigma_N^2$ (assuming ϕ_d is small) and can be used to calculate the minimum phase error variance for both 50/50 and PSA, as (see Supplement 1)

$$\sigma_{\phi_e}^2 = 3\left[\frac{\pi\Delta\nu}{P_s^2}\left(\frac{1}{2a}F_n h\nu\Delta\nu_o + 2aP_s\right)F_n h\nu\right]^{1/3}, \quad a = \begin{cases} 1, & \text{50/50} \\ 2, & \text{PSA.} \end{cases} \tag{5}$$

The corresponding locking efficiency is shown in Fig. 8(b). For larger P_s the 50/50 enjoys higher η before $\sigma_{\phi_e}^2$ becomes equal for the two cases (at $P_s = F_n h\nu\Delta\nu_o/8$, here =-59.6 dBm) after which the PSA can reach higher η for lower P_s. In fact, had we added a polarizer between the optical filter and the PD for the 50/50 it would have aligned with the PSA η in the low P_s limit due to the halving of the optical noise-noise beating power in the PD. Eq. (5) and Fig. 8(b) serve as the theoretical limits of what is possible to achieve depending on received signal power and laser linewidth for the OPLL.

Optics EXPRESS

6. Discussion and conclusion

Using a dither-based local pump locking scheme we have demonstrated phase-sensitive amplification with up to 5.7 dB sensitivity improvement w.r.t. received signal power (or 2.7 dB NF-reduction) versus the investigated phase-insensitive case.

The effect of loop delay, which was observed to be detrimental to the performance by both measured and simulated results of the 50/50 case, was identified as a limiting factor for our 600 m long PSA. Our numerical simulations were verified accurate w.r.t. experimental results and allows us to to predict the local pump PSA performance under improved conditions. For a 600 m PSA it is predicted that the use of lower phase noise lasers can improve the PSA performance, e.g. reaching <0.05 dB sensitivity penalty vs. the ideal PSA case when using $\Delta\nu$<10 Hz linewidth lasers. Moreover, in the case of a significantly shorter PSA, for instance, an integrated solution [28], we predict that the same <0.05 dB sensitivity penalty can be reached with lasers such as those used in this work ($\Delta\nu \sim 100$ Hz). Finally, theoretical limits in the zero-loop delay case were also provided.

In terms of received signal powers, the OPLL is demonstrated to maintain phase-lock down to -64 dBm which provides a significant power margin to that required by the data communication itself at the investigated symbol rate (10 GBaud QPSK). For higher symbol rates and consequently higher received powers this margin will grow whereas for much lower received powers the OPLL noise bandwidth will limit the OPLL operation.

In contrast to previous PSA demonstrations [5,15], our system is not penalized by an extra Tx pump carrier reference nor any signal power tap before the PSA. This alleviates both the complexity associated with these solutions as well as the overall "black-box" NF. The NF-penalty of our local pump solution is dictated by the achieved locking efficiency ($F_\eta = 1/\eta$) only. The phase dithering, which comprises the power "loss" in a dither OPLL, is already accounted for in this efficiency and is a parameter of optimization that provides an extra degree of freedom when designing the OPLL. Although the PSA delay provides a more challenging phase-lock than that of regular OPLLs or injection locking this can be alleviated by improved platforms and equipment.

In conclusion, the demonstrated work provides a simplified and efficient solution with great potential for frequency and phase alignment of signal, idler, and pump waves in shorter PSAs. Not needing to transmit a weak pump reference wave further enables other signal and idler-transmitting schemes such as optical frequency combs and makes PSAs more attractive in fiber- and space communication links.

Funding. Vetenskapsrådet (VR-2015-00535).

Acknowledgments. We would like to thank R. Kakarla for suggesting an early concept of local pump generation based on four-wave mixing in a PSA, T. Wik for control theory discussions, and A. Mirani and Z. He for assistance.

Disclosures. The authors declare no conflicts of interest.

Data availability. Data underlying the results presented in this paper are available in Ref. [29].

Supplemental document. See Supplement 1 for supporting content.

References

1. C. M. Caves, "Quantum limits on noise in linear amplifiers," Phys. Rev. D **26**(8), 1817–1839 (1982).
2. S. L. I. Olsson, B. Corcoran, C. Lundström, T. A. Eriksson, M. Karlsson, and P. A. Andrekson, "Phase-sensitive amplified transmission links for improved sensitivity and nonlinearity tolerance," J. Lightwave Technol. **33**(3), 710–721 (2015).
3. K. Vijayan, B. Foo, M. Karlsson, and P. A. Andrekson, "Cross-phase modulation mitigation in phase-sensitive amplifier links," IEEE Photonics Technol. Lett. **31**(21), 1733–1736 (2019).
4. P. A. Andrekson and M. Karlsson, "Fiber-based phase-sensitive optical amplifiers and their applications," Adv. Opt. Photonics **12**(2), 367–428 (2020).
5. R. Kakarla, J. Schröder, and P. A. Andrekson, "One photon-per-bit receiver using near-noiseless phase-sensitive amplification," Light: Sci. Appl. **9**(1), 153–157 (2020).

Optics EXPRESS

6. K. Vijayan, A. Mirani, J. Schröder, M. Karlsson, and P. Andrekson, "Capacity of phase-sensitively preamplified optical links at low signal-to-noise ratio," in *European Conference on Optical Communication* (Optica Publishing Group, 2022), paper We4D.2.
7. R. Slavík, F. Parmigiani, J. Kakande, C. Lundström, M. Sjödin, P. A. Andrekson, R. Weerasuriya, S. Sygletos, A. D. Ellis, L. Grüner-Nielsen, D. Jakobsen, S. Herstrøm, R. Phelan, J. O'Gorman, A. Bogris, D. Syvridis, S. Dasgupta, P. Petropoulos, and D. J. Richardson, "All-optical phase and amplitude regenerator for next-generation telecommunications systems," Nat. Photonics **4**(10), 690–695 (2010).
8. A. Tersigni, V. Calle, A. Clausen, L. K. Oxenløwe, J. Mørk, and P. Jeppesen, "Polarisation independent optical sampling using four- wave mixing," in *Conference on Lasers and Electro-Optics/Quantum Electronics and Laser Science Conference* (Optica Publishing Group, 2003), paper CMR2.
9. P. Andrekson and M. Westlund, "Nonlinear optical fiber based high resolution all-optical waveform sampling," Laser Photonics Rev. **1**, 231–248 (2007).
10. K. J. Lee, F. Parmigiani, S. Liu, J. Kakande, P. Petropoulos, K. Gallo, and D. Richardson, "Phase sensitive amplification based on quadratic cascading in a periodically poled lithium niobate waveguide," Opt. Express **17**(22), 20393–20400 (2009).
11. Z. Tong, C. Lundström, P. A. Andrekson, M. Karlsson, and A. Bogris, "Ultralow noise, broadband phase-sensitive optical amplifiers, and their applications," IEEE J. Sel. Top. Quantum Electron. **18**(2), 1016–1032 (2012).
12. Z. Tong, C. Lundström, P. A. Andrekson, C. J. McKinstrie, M. Karlsson, D. J. Blessing, E. Tipsuwannakul, B. J. Puttnam, H. Toda, and L. Grüner-Nielsen, "Towards ultrasensitive optical links enabled by low-noise phase-sensitive amplifiers," Nat. Photonics **5**(7), 430–436 (2011).
13. R. Kakarla, J. Schröder, and P. A. Andrekson, "Optical injection locking at sub nano-watt powers," Opt. Lett. **43**(23), 5769–5772 (2018).
14. R. Larsson, K. Vijayan, and P. A. Andrekson, "Zero-offset frequency locking of lasers at ultra-low optical powers," in *Optical Fiber Communication Conference* (Optica Publishing Group, 2023), paper Th4A.5.
15. S. Shimizu, T. Kazama, T. Kobayashi, T. Umeki, K. Enbutsu, R. Kasahara, and Y. Miyamoto, "Non-degenerate phase-sensitive amplification scheme using digital dispersion pre-equalization for unrepeated transmission," Opt. Express **29**(6), 8451–8461 (2021).
16. L. Kazovsky, "Decision-driven phase-locked loop for optical homodyne receivers: Performance analysis and laser linewidth requirements," J. Lightwave Technol. **3**(6), 1238–1247 (1985).
17. F. Herzog, K. Kudielka, D. Erni, and W. Bachtold, "Optical phase locking by local oscillator phase dithering," IEEE J. Quantum Electron. **42**(10), 973–985 (2006).
18. M. L. Stevens, D. O. Caplan, B. Robinson, D. M. Boroson, and A. L. Kachelmyer, "Optical homodyne PSK demonstration of 1.5 photons per bit at 156 Mbps with rate-$\frac{1}{2}$ turbo coding," Opt. Express **16**(14), 10412–10420 (2008).
19. C. Yue, J. Li, J. Sun, R. Zhu, X. Hou, X. Zhang, L. Liu, and W. Chen, "Homodyne coherent optical receiver for intersatellite communication," Appl. Opt. **57**(27), 7915–7923 (2018).
20. Y. Yang, C. Geng, F. Li, G. Huang, and X. Li, "Multi-aperture all-fiber active coherent beam combining for free-space optical communication receivers," Opt. Express **25**(22), 27519–27532 (2017).
21. K. Balakier, L. Ponnampalam, M. J. Fice, C. C. Renaud, and A. J. Seeds, "Integrated semiconductor laser optical phase lock loops," IEEE J. Sel. Top. Quantum Electron. **24**(1), 1–12 (2018).
22. R. Larsson, K. Vijayan, J. Schröder, and P. A. Andrekson, "Low-noise phase-sensitive optical parametric amplifier with local pump generation using digital frequency and phase control," in *Optical Fiber Communication Conference* (Optica Publishing Group, 2023), paper Th1B.4.
23. Y. Shaked, Y. Michael, R. Z. Vered, L. Bello, M. Rosenbluh, and A. Pe'er, "Lifting the bandwidth limit of optical homodyne measurement with broadband parametric amplification," Nat. Commun. **9**(1), 609 (2018).
24. "RedPitaya, Swiss Army Knife For Engineers," (2022).
25. C. Madsen, "Boundless-range optical phase modulator for high-speed frequency-shift and heterodyne applications," J. Lightwave Technol. **24**(7), 2760–2767 (2006).
26. S. J. Savory, "Digital filters for coherent optical receivers," Opt. Express **16**(2), 804–817 (2008).
27. W. Ma, B. Xiong, C. Sun, X. Ke, Z. Hao, L. Wang, J. Wang, Y. Han, H. Li, and Y. Luo, "Laser frequency noise characterization by self-heterodyne with both long and short delay," Appl. Opt. **58**(13), 3555–3563 (2019).
28. Z. Ye, P. Zhao, K. Twayana, M. Karlsson, V. Torres-Company, and P. A. Andrekson, "Overcoming the quantum limit of optical amplification in monolithic waveguides," Sci. Adv. **7**(38), eabi8150 (2021).
29. R. Larsson, K. Vijayan, J. Schröder, and P. A. Andrekson, "Data - Low-Noise Phase-Sensitive Optical Parametric Amplifier with Lossless Local Pump Generation using a Digital Dither Optical Phase- Locked Loop, (2023)," Zenodo (2023), https://doi.org/10.5281/zenodo.8337536.